

Original scientific paper

ONE-DIMENSIONAL BIOLOGICAL MODEL OF SYNOVIAL JOINTS REGENERATIVE REHABILITATION IN OSTEOARTHRITIS

Valentin L. Popov¹, Aleksandr Poliakov², Vladimir Pakhaliuk²

¹Institute of Mechanics, Technische Universität Berlin, Berlin, Germany

²Polytechnic Institute, Sevastopol State University, Sevastopol, Russian Federation

Abstract. *This work is devoted to the study of a one-dimensional phenomenological model of a focal defect regenerative rehabilitation in the articular cartilage. The model is based on six differential equations in partial derivatives of the "Diffusion-Reaction" type, which was previously used by a number of authors to study cellular processes in various tissues under cell therapy conditions. To take into account the influence of moderate mechanical stimulation of immature tissue, an indirect approach was used, as a result of which some model parameters that directly affect cell proliferation and differentiation were varied considering experimental data. The results of the model study show that moderate stimulation of immature tissue in the early stages of repair the focal articular cartilage defect under conditions of cell therapy leads to an intensification of regenerative processes in the tissue and promotes more rapid formation of the extracellular matrix.*

Key words: *Synovial joint, Articular cartilage, Osteoarthritis, Cell therapy, Tissue engineering, Regenerative rehabilitation*

1. INTRODUCTION

The articular surfaces of long bones are covered with articular cartilage (AC), which is a type of connective tissue with an almost homogeneous structure at the macro level. However, at the micro level, AC has a complex heterogeneous structure, which is based on a hydrated elastic extracellular matrix (ECM), inside which chondrocytes are located, which are formed from chondroblasts. Slightly mobile chondrocytes, due to the ability to divide, provide the synthesis and release of ECM elements. Moreover, they are grouped in specific areas - lacunae, permeable to low molecular weight metabolites. This allows for interstitial AC growth and its potential for regeneration in the event of damage.

Received February 03, 2022 / Accepted March 21, 2022

Corresponding author: Valentin L. Popov

Institute of Mechanics, Technische Universität Berlin, Str. des 17 Juni 135, 10623 Berlin, Germany

E-mail: v.popov@tu-berlin.de

However, in AC, blood, lymphatic vessels and nerves are almost completely absent, and therefore its formation, nutrition and lubrication are carried out only due to the interstitial fluid. The regenerative AC insufficiency determined by this feature in conditions of its progressive destruction leads not only to a variety of tissue damage mechanisms, but also to a variety of morphological phenomena that determine its clinical state. Therefore, at present, treatment options for AC in the advanced stages of osteoarthritis are limited to injections of analgesics and total arthroplasty of the joints [1]. At the same time, in the early stages of osteoarthritis and in cases of focal cartilage defects, a greater number of therapies for the disease may be useful, including regenerative medicine-related cell therapy and tissue engineering strategies.

When developing new methods and strategies for the treatment of joint diseases, including osteoarthritis, it is necessary to take into account the microstructure of the AC, schematically shown in Fig.1.

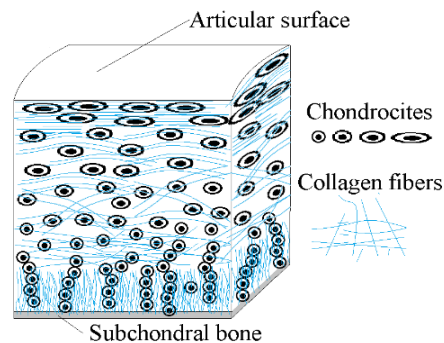


Fig. 1 Schematic cross-sectional diagram of healthy articular cartilage

First of all, this concerns its zonal structuring, which includes three non-mineralized zones: superficial, intermediate, radial (deep) and one mineralized - the so-called calcified cartilage [2]. The surface zone includes chondrocytes flat in shape, located close to each other and collagen fibers oriented along tangents to the articular surface. The structure of the intermediate zone differs significantly from the surface one. In it, chondrocytes have an oblique form of organization, and collagen fibers are scattered randomly in space. Chondrocytes of the radial zone have a spherical shape and are structured along columns, parallel to which collagen fibers are located, penetrating into the calcified cartilage, thereby ensuring anchoring of the AC on the subchondral bone [3].

Chondrocytes function under anaerobic conditions, receiving nutrients by diffusion from the interstitial fluid, and their shape can change not only depending on belonging to a particular AC zone, but also on the physiological state, level of motor activity and age of the patient [4].

To restore small-sized focal AC defects, mosaic chondroblast technologies are used using native osteochondral grafts. However, their practical applicability is limited by a number of disadvantages, such as the limited size of the defect to be repaired, the difficulty of choosing AC sites with the desired curvature for graft retrieval, the risk of postoperative pain in the joint, etc. Elimination of these shortcomings is potentially possible with the use of technologies for implantation the in vitro cultured autologous

chondrocytes (Autologous Chondrocytes Implantation (ACI)), allowing, among other things, to control the process of reparative regeneration of the damaged AC in order to fully restore it. However, chondrocytes undergo dedifferentiation during cultivation and reproduction, as a result of which the expression of chondrocyte markers (collagen II, aggrecan, transcription factor SOX9) decreases, and the expression of fibroblast markers (collagen I, versican) increases [5]. As a result, cells acquire a fibroblast-like phenotype and become unable to produce the components necessary for AC repair. This is a significant challenge in the development of ACI technologies. One of the ways to solve it is to select a different type of cells for implantation into the damaged area of the AC, capable of differentiating into articular chondrocytes.

It is known that stem cells possess the properties of self-renewal and differentiation into various cell lines. Therefore, in modern cell technologies focused on the restoration of not only focal, but also extensive AC defects, mesenchymal stem cells (MSC) and embryonic stem cells (ESC) (Articular Stem cell Implantation (ASI)) are used, which meet the criteria established by The International Society for Cellular Therapy's Mesenchymal Stromal Cell Committee (ISCT MSC) [6]. The process of differentiation of progenitor cells into a specific cell line can be controlled by regulatory genes. But the population of cells obtained in this way, as a rule, does not fully correspond to the target tissue in terms of its biochemical and biomechanical properties [7]. This discrepancy can be eliminated by implanting an artificial extracellular matrix (scaffold) into the defect area along with MSC / ESC. This approach is often used in modern AC recovery technologies. In this case, the scaffold is chosen so that its structure facilitates the creation of an environment in which cells could modulate their environment *in vitro* and / or *in vivo*, just as it happens in the target tissue [8]. Therefore, in addition to the desired structure, the scaffold must have mechanical properties corresponding to the properties of the target tissue [9].

Growth factors that function as signaling molecules that determine intercellular interactions and processes are of great importance for the development of new methods and strategies for AC treating. For example, fibroblast growth factors (FGFs) play a key role in the proliferation and differentiation of a wide range of cells and tissues; bone morphogenetic proteins (BMP), which form a group of multifunctional growth and regeneration factors belonging to the transforming growth factor TGF- β superfamily, are able to regulate various cellular processes in the body. In healthy AC, the growth factors FGF-1 and BMP-2 provide the metabolism and renewal of chondrocytes. Extensive information about these molecules, their role in metabolism and regulation of molecular processes of cartilage tissue remodeling is given in numerous literatures [10-18].

It is obvious that innovative strategies for the treatment of AC, including those focused on the complete restoration of damaged tissue areas, should be built taking into account the conditions and the nature of the synovial joint operating as a whole, enduring the action of significant loads. So, for example, the load perceived by a healthy knee joint when a person climbs stairs is 8-10 times greater than his body weight and AC resists it without destruction. The synovial joint elements, touching along the articular surfaces, are subjected to compression, shear and sliding relative to each other in the process of their operating. Since AC has a very low permeability, during compression, the hydrostatic pressure of the interstitial fluid present in it increases rapidly, allowing the AC to take on external stress. As the compressive load increases, interstitial fluid begins to be released from the AC, which leads to a redistribution of some of the load on the solid ECM and to its consolidation. Upon reaching equilibrium, the flow of interstitial fluid from the AC

stops, and the ECM takes over the entire load [19]. This effect is known as stress relaxation in AC and characterizes one of its most important characteristics, which determine the compression process and support functions [20].

Along with viscoelastic properties, stress relaxation in AC is quite convincingly explained on the basis of its two-phase model, in which it is assumed that AC contains a small number of cells (~ 1% of the tissue mass) and its mechanical performances are mainly determined by ECM, which consists of liquid and solid phases [21]. The liquid phase (~ 80% by weight) is represented by interstitial fluid, and the composite solid phase, as a porous, permeable material bound to fibers, is represented by macromolecules, among which collagen II and complex proteins - proteoglycans, predominate. If we do not take into account the biochemical processes and cellular changes occurring in the cartilaginous tissue during normal operating under the development of pathology or regeneration, then taking into account the above-mentioned features, AC can be considered as a continuous poroelastic medium and according to the theory of effective poroelasticity of M.A. Biot [22, 23], to create and investigate various models of cartilage tissue within the framework of continuum mechanics. Models considering other characteristic features of AC in synovial joint make it possible to study the interaction of several tissues on each other, cell-cell or cell-ECM interactions, as well as the processes of migration, differentiation and natural cell death. For example, M. Blewis and colleagues used the synovial joint (SJ) compartment model to predict the dynamic processes occurring in the interstitial fluid [24]. Taking into account the mass balance of hyaluronic acid and proteoglycan-4 in synovial fluid, the authors reduced the problem to a system of linear differential equations with three state variables, considering the rate of secretion, decomposition and fluid flow through the synovial membrane. The performances of the model compartments used by the authors can be changed if the characteristics of the synovial fluid change, therefore it is applicable for the analysis of normal and pathological conditions of the joint, as well as for conditions caused by certain therapeutic procedures, for example, hyaluronic acid injections, MSC / ESC and etc.

More complex models are also known, including those applicable to the analysis of rheumatoid arthritis of the joint, depending on changes in the state of inflammatory cells, endothelium, fibroblasts, chondrocytes, cytokines, and growth factors in the SJ compartment [25]. That is, the analysis of AC within synovial joint *in silico* makes it possible to investigate and predict the physiological state, structural rearrangement, cellular and chemical processes occurring in tissues from different points of view. It seems that the results of such studies, as well as a lot of experimental data, contributed to the accumulation of a critical amount of knowledge necessary to create effective technologies for the treatment of various synovial joint diseases. However, up to the present time, such technologies have not yet been created. At the same time, it should be noted that in recent years there has been significant progress in this area of medical science. Methods for cultivating and storing cells for therapeutic use, as well as methods for their transplantation, are being improved. Tissue engineering is evolving towards the creation of biomimetic and more complex tissue engineering constructs (including those with the desired shape) that could be used to replace larger sections of damaged AC. However, even the use of such modern high-tech methods in many clinical cases does not lead to successful treatment of osteoarthritis, and this fact is the main motive for finding new ways to combat this disease. One of the new areas of medical science, within which an effective solution to the problem of AC recovery can be found, is regenerative rehabilitation, which is based on the combination

of modern technologies of regenerative and rehabilitation medicine [26-28]. Many theoretical and experimental results testify to the synergistic effect that can potentially be achieved as a result of such a combination.

From the point of view of regenerative rehabilitation, of interest are studies that have studied the responses of cartilage tissue, cells, and molecules to the action of mechanical stimuli. It has been established that optimal mechanical stimulation promotes collagen formation, cell viability, and fiber organization in tissue engineering constructs [29, 30]. In vitro experiments indicate that both short-term and long-term compressive and/or shear loads change the composition of cartilage tissue [31], its structure [32], and function [33]. During daily physical activity, mechanical signals resulting from the load on the joints and the corresponding deformation of the articular tissues modulate the metabolism of chondrocytes and cause coordinated changes in the biochemical and mechanical properties of AC [34-36]. At the same time, normal cartilage homeostasis is partially associated with cyclic loads that ensure the activation of ECM-associated growth factor TGF- β (BMP-2) [37, 38]. FGF-1 synthesis also presumably depends on the amplitude and frequency of the stimulating force acting on the AC, which increases angiogenesis in the subchondral bone [39] and, consequently, promotes cartilage tissue regeneration. It is generally accepted that mechanical stimulation strongly influences the mechanical properties of the superficial AC zone [40], but is enzymatically regulated in deeper zones [41, 42]. Moreover, as shown in [43], it is very likely that the central channel for the transformation of mechanical forces into biological reactions in AC is the MAPK (mitogen-activated protein kinase) pathway.

The effects described very briefly above, which deserve a detailed systematic study, indicate that regenerative rehabilitation technologies that use AC mechanical stimulation in vivo along with cell therapy and tissue engineering strategies may be effective in the treatment of various synovial joint diseases, including osteoarthritis [44]. For their development, various resources should be involved, including simulation and in silico studies of processes occurring in AC under various conditions, under various tissue conditions and types of stimulation, since there is still no complete understanding of the mechanisms by which mechanical stimulation promotes joint homeostasis, chondroprotection, and the production of pro-inflammatory mediators. Such models can be different in form and content, including biological, biophysical, biochemical, biomechanical and combined. In this paper, we investigate one-dimensional biological models of repair the AC focal defects based on the strategies of cell therapy and regenerative rehabilitation in order to compare, first of all, the qualitative results of these strategies implementation.

2. DESCRIPTION OF THE MODEL

Most of the mathematical models of biological processes in tissues are designed to analyze a relatively small number of related state variables that are most important for the researcher in solving a specific problem. This is explained by the fact that, by their nature, biological tissues are pronounced homeostatic systems, with their inherent unpredictability, instability and striving for balance. In this regard, the processes occurring in them are very variable and depend on many factors, often not completely defined or even random. In addition, even small changes in the internal parameters of a particular tissue can lead to a qualitative restructuring of its homeostasis, i.e. to a bifurcation. Therefore, complex

multifactorial mathematical models of tissue processes can be studied only in stable regions of the space of state variables, the determination of which is a separate rather complicated problem. But important information can also be obtained by studying simplified models of tissue processes, in which some important variables and parameters are taken into account indirectly. As examples, here are a number of models tested in the study of wound healing and bone fractures [45]. In this work, we use a simplified phenomenological biological model built on the basis of the “Diffusion-Reaction” type system of equations to simulate cellular therapy and regenerative rehabilitation of AC focal defect. Previously, such models were used by M. Lutianov et al. [46] and later (with some variations) by K. Campbell et al. [47, 48] to study various AC regeneration strategies under cell therapy. When substantiating them, the authors used the approach proposed by A. Bailón-Plaza and M.C. van der Meulen to study the effect of growth factors on the healing of bone fractures [49], based on modeling the diffusion migration of cells and the reaction of the environment that promotes their proliferation, differentiation, and death.

Since the biological processes of cartilage tissue repair and bone tissue fracture healing have a common basis, their biological models can be considered similar. Therefore, following [46], the biological model of regenerative rehabilitation of AC focal defect can be represented as a system of partial differential equations with variables: C_S is the MSC density; C_C is the chondrocyte density; n is the nutrient concentration; m is the ECM density:

$$\frac{\partial C_S}{\partial t} = \underbrace{\nabla[D_S \nabla C_S]}_{diffusion} + \underbrace{p_1 C_S \frac{n}{n+n_0} H(n-n_1)}_{proliferation} - \underbrace{p_2 C_S H(C_S - C_{S0})}_{differentiation} - \underbrace{p_3 C_S H(n_1 - n)}_{death}, \quad (1a)$$

$$\frac{\partial C_C}{\partial t} = \underbrace{\nabla[D_C \nabla C_C]}_{diffusion} + \underbrace{p_4 C_C \frac{n}{n+n_0} H(n-n_1)}_{proliferation} + \underbrace{p_2 C_S H(C_S - C_{S0})}_{differentiation} - \underbrace{p_5 C_C H(n_1 - n)}_{death}, \quad (1b)$$

$$\frac{\partial n}{\partial t} = \underbrace{\nabla[D_n \nabla n]}_{diffusion} - \underbrace{\frac{n}{n+n_0} (p_6 C_S + p_7 C_C)}_{reaction}, \quad (1c)$$

$$\frac{\partial m}{\partial t} = \underbrace{\nabla[D_m \nabla m]}_{diffusion} + \underbrace{p_8 \frac{n}{n+n_0} C_C}_{reaction}, \quad (1d)$$

which, if necessary, can be supplemented by equations with variables: g is the concentration of growth factors FGF-1 and b is the concentration of growth factors BMP-2 [47]:

$$\frac{\partial g}{\partial t} = \underbrace{\nabla[D_g \nabla g]}_{diffusion} + \underbrace{p_9 C_S - p_{11} g}_{reaction}, \quad (2a)$$

$$\frac{\partial b}{\partial t} = \underbrace{\nabla[D_b \nabla b]}_{diffusion} + \underbrace{p_{12} C_C - p_{13} g}_{reaction}, \quad (2b)$$

where $\nabla = \frac{\partial}{\partial x} \vec{i} + \frac{\partial}{\partial y} \vec{j} + \frac{\partial}{\partial z} \vec{k}$; $\nabla \varphi(x, y, z) = \frac{\partial \varphi}{\partial x} \vec{i} + \frac{\partial \varphi}{\partial y} \vec{j} + \frac{\partial \varphi}{\partial z} \vec{k} = \overrightarrow{grad} \varphi$;

$\nabla \overrightarrow{grad} \varphi = \text{div} \overrightarrow{grad} \varphi = \frac{\partial^2 \varphi}{\partial x^2} + \frac{\partial^2 \varphi}{\partial y^2} + \frac{\partial^2 \varphi}{\partial z^2}$; $\varphi(x, y, z)$ is a some scalar function.

Descriptions of the variables and constant parameters of the model included in Eqs (1a – 1d) and (2a – 2b), as well as their possible values in dimensional and dimensionless

form, are given in Appendix A. Previously, these values were established experimentally or justified theoretically and used in a number of works on bone fracture healing, implant osseointegration, and AC repair [46-51]. Considering the fact that the main goal of this work is to study, first of all, the qualitative results of the various AC recovery strategies implementation, the models of which are characterized by significant uncertainty and depend on many factors, including the physiological state of the intended patient, the nature of the defect, the method of tissue stimulation, etc., these data were used only as estimates of the parameters. In addition, we assumed that mechanical stimulation of AC in the vicinity of the reconstructed region changes the mechanical state of the medium, which also leads to a change in the values of the model parameters. Since tissues respond differently to various physiological loads and to stimuli of different types and intensities [52], hypothetically, such changes should lead either to an improvement or deterioration in the processes of damaged tissues repair. In this regard, when modeling, we varied the values of the parameters that change under the influence of mechanical stimuli, taking into account the results of numerous studies available in the literature.

As a criterion for the quality of AC repair processes, we used the final density distribution of the synthesized ECM in the region of the repaired AC defect. To evaluate other indicators achieved as a result of the recovery processes implementation, including the phenotype of the resulting tissue, biomechanical models are more suitable, including equations that describe the stress-strain state of the tissue during stimulation [53–55].

To take into account the mechanical stimulation of AC in the process of regenerative rehabilitation, we used the approach proposed by A. Andreykiv et al. to model the healing of bone fractures with mechanoregulation of cell differentiation and proliferation [56]. In their model, the authors consider the fact that the diffusion coefficients (D_m, D_f) and proliferation rates (P_m, P_f) of MSC and fibroblasts, respectively, depend on the volume concentration of the bone (m_b) and cartilage (m_c) fractions of the ECM. At the same time, the initial values of proliferation rates (P_{m0}, P_{f0}) were calculated in accordance with the mechanoregulation index [53]

$$S = \frac{\gamma}{a} + \frac{v}{b},$$

where γ and v are the maximum shear stress and maximum velocity of the interstitial fluid, respectively, and a and b are constants [57].

According to the hypothesis proposed in [53], if S is less than a certain threshold value S_{min} , then the mechanical environment of the tissue is favorable for osteoblast differentiation and bone tissue synthesis, and at moderate values ($S_{min} < S < S_{max}$), that do not exceed some maximum value S_{max} , the environment favor the differentiation of chondrocytes and the formation of cartilaginous tissue. And, finally, high values of the index ($S > S_{max}$) contribute to the differentiation of fibroblasts and the formation of fibrous tissue in the area of the bone fracture. Therefore, in the model [56], the rates of differentiation of fibroblasts, chondrocytes, and osteoblasts (P_f, P_c, P_b) were also calculated depending on the value of the mechanoregulation index S .

Thus, the approach described above makes it possible to indirectly take into account the effect of mechanical stimulation on tissue formation in the process of regenerative rehabilitation. Moreover, if we take into account the results of experiments, according to which low-amplitude cyclic tissue deformation leads to an increase in osteoblast proliferation

by about 1.5 times [58, 59], and also that unstimulated chondrocytes proliferate at a rate similar to osteoblasts [60, 61], a qualitative analysis of the AC regenerative rehabilitation process can be performed by varying the values of cell proliferation and differentiation coefficients without calculating the mechanoregulation index. It should also be noted that during AC repair, bone formation is almost impossible, but there is a possibility of fibrous tissue formation. But with moderate stimulation, according to the hypothesis described above [53], this probability is very small.

Figure 1 is a schematic representation of the repair process for an AC focal defect using ACI/ASI cellular technologies and/or regenerative rehabilitation, which shows a schematic cross-section of the defect on an enlarged scale. It is assumed that the defect has small dimensions in width and its properties in planes perpendicular to the defect practically do not change, which allows us to consider this problem as one-dimensional. The origin of the coordinate system is located on the subchondral bone, and the x coordinate axis is directed towards the articular surface. The subchondral bone is considered permeable, and MSC can diffuse from it into the defect, the flow of which is determined by a certain time function $f(t)$. The fluxes from the subchondral bone of chondrocytes, growth factors, nutrients, and ECM elements are assumed to be zero, although they can also be specified as specific functions of time if necessary. Thus, the boundary conditions at the point $x = 0$ look like:

$$-D_S \frac{\partial c_S}{\partial x} = f(t), \quad D_C \frac{\partial c_C}{\partial x} = 0, \quad D_g \frac{\partial g}{\partial x} = 0, \quad D_b \frac{\partial b}{\partial x} = 0, \quad D_n \frac{\partial n}{\partial x} = 0, \quad D_m \frac{\partial m}{\partial x} = 0. \quad (3)$$

Boundary conditions on the defect surface at $x = d$:

$$D_S \frac{\partial c_S}{\partial x} = 0, \quad D_C \frac{\partial c_C}{\partial x} = 0, \quad D_g \frac{\partial g}{\partial x} = -\gamma g, \quad D_b \frac{\partial b}{\partial x} = -\chi b, \quad n = N_0, \quad D_m \frac{\partial m}{\partial x} = 0. \quad (4)$$

That is, it is assumed that the fluxes of MSCs, chondrocytes, and ECM elements on the surface of the defect are equal to zero, and nutrients with a constant concentration of N_0 enter the defect from the synovial fluid. The flows of growth factors in the study of the model (1a – 1d, 2a – 2b) calculated in proportion to their concentrations with the coefficients γ and χ , respectively.

The initial conditions of the problem are formulated in accordance with a certain strategy of regenerative rehabilitation. For example, when implementing the ASI strategy, it is assumed that MSCs are implanted into a defect, and the cells are arranged according to the height of the defect according to a certain law $C_S(0) = C_S^{(0)}h(x)$. If at the same time a scaffold is implanted into the defect, then the initial ECM density taken equal to $(0) = m_3 + m_s$, where m_3 is the initial ECM density and m_s is the scaffold density. Then, taking into account the density of nutrients $n(0) = N_0$ and zero values of other state variables at the initial moment of time, the initial conditions have the following form:

$$C_S = C_S^{(0)}h(x), \quad g(0) = 0, \quad b(0) = 0, \quad C_C = 0, \quad n(0) = N_0, \quad m(0) = m_3 + m_s, \quad (5)$$

where $C_S^{(0)}$ is the initial MSC density.

The initial conditions corresponding to other AC focal defect restoration strategies are formed in a similar way.

The scheme displayed in Figure 2 can also be used to describe the process of AC regenerative rehabilitation. In this case, in addition to the conditions of cell therapy and tissue engineering strategies, the effect of stimulating effects on tissue repair should be

taken into account. At the same time, one should consider the fact that ASI/ACI technologies involve implantation of MSC/ESC and/or autologous chondrocytes into the area of the defect. In the case of implementing tissue engineering strategies, cells are pre-seeded *in vitro* on an artificial matrix - scaffold, in order to increase their viability, proliferation, osteogenic and chondrogenic signal expression.

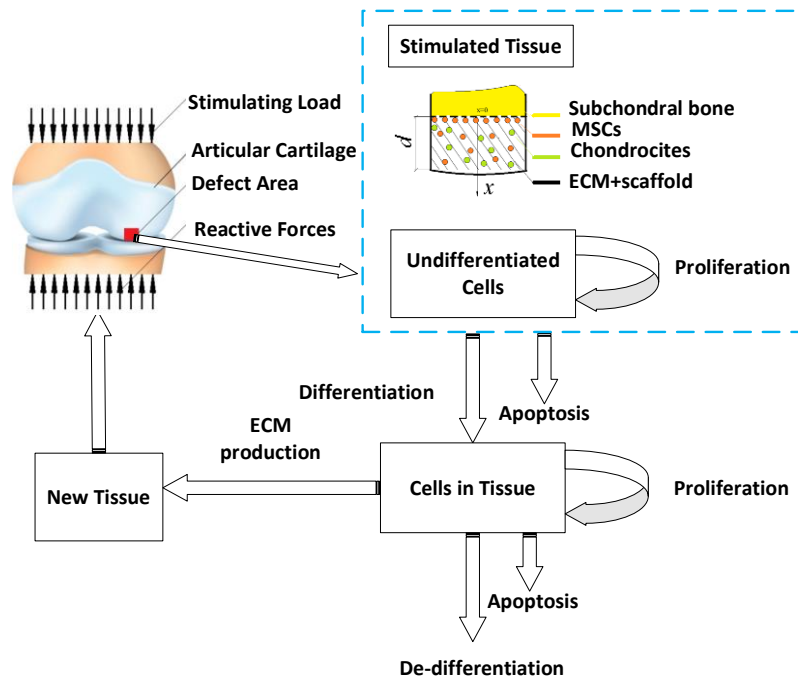


Fig. 2 Scheme of AC focal defect repair process using ACI/ASI cellular technologies and regenerative rehabilitation

The results of a systematic study of AC recovery strategies using ASI/ACI models, including various combinations of them, are presented in [47, 48]. As a quality criterion for choosing the percentage of implanted cells (MSC and autologous chondrocytes), the authors used the average density of the ECM formed new tissue. It has been shown that, in principle, each of the possible strategies (100% ASI; 90% ASI + 10% ACI; ...; 10% ASI + 90% ACI; 100% ACI) can be effective. However, from a practical point of view, the effectiveness of AC damage repair technology is also evaluated taking into account the availability of cell types, the overall cost and the effectiveness of the procedure. In this regard, in this study, ASI technology (100% ASI) was adopted as a standard strategy for cell therapy. That is, we assume that regenerative rehabilitation strategies that involve moderate mechanical stimulation of immature tissue in the damaged area of the AC will contribute to its recovery in all practically significant cases.

The study of the AC focal defects restoration processes was carried out using a mathematical model (1a – 1d, 2a – 2b) for various parameter values. Based on the hypothesis, confirmed by numerous experimental data, it is possible to select such stimulating effects that

would enhance the effects of cell therapy and contribute to the creation of the best conditions for the restoration of damaged tissue in vivo. The solution of this problem would contribute to the development of the best strategies for the regenerative rehabilitation of tissues damaged due to injuries or diseases, including osteoarthritis.

The scheme (Fig. 2) shows that stimulated tissue cells can proliferate, differentiate into chondrocytes, and die. Therefore, the main goal of stimulating immature tissue in the area of the AC defect is to provide the best conditions for the viability and differentiation of progenitor cells into chondrocytes, which would promote the production of ECM and the formation of new tissue with the desired phenotype. In this study, we took into account the effect of mechanical stimulation of immature tissue by increasing the coefficients: p_{4_0} is a chondrocyte proliferation constant, $p_{4_{00}}$ is a chondrocyte proliferation rate (from FGF-1) and p_2 is a MSC differentiation rate, because p_{4_0} and $p_{4_{00}}$ determine the amplitude value of the chondrocyte proliferation rate:

$$p_4 = B_m \left(1 - \frac{c_c}{c_{cmax}}\right) = \left(p_{4_0} \frac{m}{m^2 + m_2^2} + p_{4_{00}} \frac{g}{g + g_0}\right) \left(1 - \frac{c_c}{c_{cmax}}\right),$$

and p_2 in Eq. (1b) determines the modulus of the chondrocyte differentiation rate:

$$V_{dCh} = p_2 C_S H(C_S - C_{S_0}),$$

where $(C_S - C_{S_0}) = \begin{cases} 0, & C_S \leq C_{S_0} \\ 1, & C_S > C_{S_0} \end{cases}$ is the Heaviside function,

$C_{S_0} = (C_{S_{0max}} - C_{S_{0min}})e^{-\alpha b}$ is a MSC threshold density,

$C_{S_{0max}}$ is a maximum threshold density, $C_{S_{0min}}$ is a minimum threshold density, α is a threshold MSC density reduction factor.

Following [58-61], when simulation processes of regenerative rehabilitation of AC, the values of these coefficients were taken to be 1.5 times greater than their estimated values given in Appendix A. It is clear that such an approach does not allow making any quantitative estimates that could be used in medical practice. But it allows one to obtain and compare qualitative estimates of various AC defect recovery strategies.

3. RESULTS AND DISCUSSION

Solutions to the equations system (1a – 1d, 2a – 2b) for various model parameters were obtained in a dimensionless form by the finite element method in Matlab R2021b (MathWorks, USA) using the *pdepe* function. The dimensionless values of the parameters were calculated taking into account the characteristic values that determine the main features of the model: $d = 2 \text{ mm}$ is a defect thickness/depth; $C_{total,max_0} = 10^6 \frac{Nc}{mm^3}$ is a maximum total cell density; $m_{max} = 10^{-4} \frac{g}{mm^3}$ is a maximum ECM density; $N_0 = 6.5 \times 10^{-11} \frac{Nm}{mm^3}$ is an initial nutrient concentration; $p_{8_0} = 3.75 \times 10^{-13} \frac{g}{mm^3} \cdot \frac{1}{\frac{Nc}{mm^3}} \cdot \frac{1}{hour}$ is an ECM production constant; $g_0 = 10^{-10} \frac{g}{mm^3}$ is a FGF-1 reference concentration; $b_0 = 10^{-10} \frac{g}{mm^3}$ is a BMP-2 reference concentration. The dimensionless time was determined by the formula $\tilde{t} = t \frac{p_{8_0} C_{total,max_0}}{m_{max}}$, according to which the time unit corresponds to about 11 days [48]. Dimensionless values of other model parameters are presented in Appendix A.

Fig. 3 shows the evolution of ECM density of the formed tissue under standard ASI conditions, and Fig. 4 shows the evolution of ECM density, chondrocytes population density, MSC population density, BMP-2 concentration and FGF-1 concentration over time with the values of the model parameters given in the Appendix A. Similar graphs obtained under the conditions of regenerative rehabilitation of the AC injured area under the respective parameter values justified above are shown in Figs 5 and 6, respectively.

The simulation results indicate that the process of ECM formation occurs in the same way when implementing two AC recovery strategies studied in this work. However, within the framework of the model under study, in the early stages, the maximum values of ECM density are achieved at different points in time (see Figs 3 and 5). Nevertheless, in all cases, the regenerative rehabilitation strategy provides better conditions for the AC defect repair compared to the ASI strategy. So from Figs 3 and 5 it follows that ECM density at all stages of evolution is of greater importance in terms of regenerative rehabilitation (Table 1). An analysis of the evolution of other model state variables indicates that their maximum values are also reached at different points in time when implementing different strategies (see Table 2). In addition, it should be noted that under conditions of regenerative rehabilitation, the maximum values of MSC population density and FGF-1 concentration have lower values under ASI conditions (see Table 3). This is explained by the property of the model (1a – 1d, 2a – 2b), which consists in the fact that during regenerative rehabilitation, part of the MSC population differentiates into chondrocytes and this process is accompanied by a decrease in growth factors FGF-1.

Table 1 ECM density values at various stages of AC recovery

| Strategy | time, <i>t</i> | | |
|-----------------------------|----------------|----------|----------|
| | 6 | 11 | 16 |
| | ECM density | | |
| AC | 0.066150 | 0.425962 | 0.470151 |
| Regenerative Rehabilitation | 0.084656 | 0.469820 | 0.486250 |

Table 2 Time to reach the maximum values of the model state variables (Figs 4 and 6)

| Strategy | Model state variable | | | | |
|-----------------------------|--|----------------------|------------------------|---------------------|---------------------|
| | ECM density | Chondrocytes density | MSC population density | BMP-2 concentration | FGF-1 concentration |
| | time, <i>t</i> (<i>t</i> = 1 roughly equivalent to 11 days) | | | | |
| ASI | 16 | 2.21 | 0.55 | 3.31 | 1.66 |
| Regenerative Rehabilitation | 16 | 2.21 | 0.55 | 2.76 | 1.03 |

Table 3 Maximum values of the model state variables for the entire time of evolution (according to Figs 4 and 6)

| Strategy | Model state variable | | | | |
|-----------------------------|----------------------|----------------------|------------------------|---------------------|---------------------|
| | ECM density | Chondrocytes density | MSC population density | BMP-2 concentration | FGF-1 concentration |
| ASI | 0.470151 | 221.441 | 486.656 | 94.851 | 114.479 |
| Regenerative Rehabilitation | 0.48625 | 260.617 | 415.215 | 114.788 | 94.446 |

And, finally, it should be noted that the constant parameters of the model contribute to the fact that at a certain point in time the ECM is saturated and its density subsequently practically does not change in the positive direction of the x axis (see Figs 7 and 8). However, the saturation process is reoriented in the opposite direction, which leads to an increase in density in areas located closer to the subchondral bone. Predicting the further process of matrix transformation is quite difficult (if at all possible), since the model we use does not take into account many factors that affect the AC recovery process.

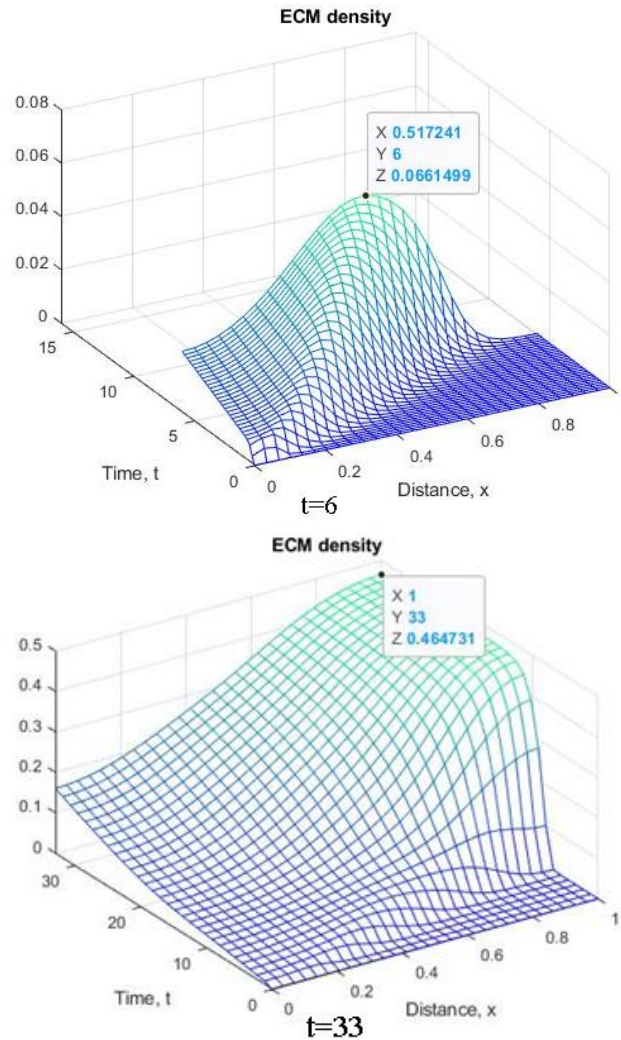


Fig. 3 The evolution of ECM density $m=m(x,t)$ of the formed tissue under standard ASI conditions ($t=1$ roughly equivalent to 11 days; $x=1$ equivalent to $d=2$ mm)

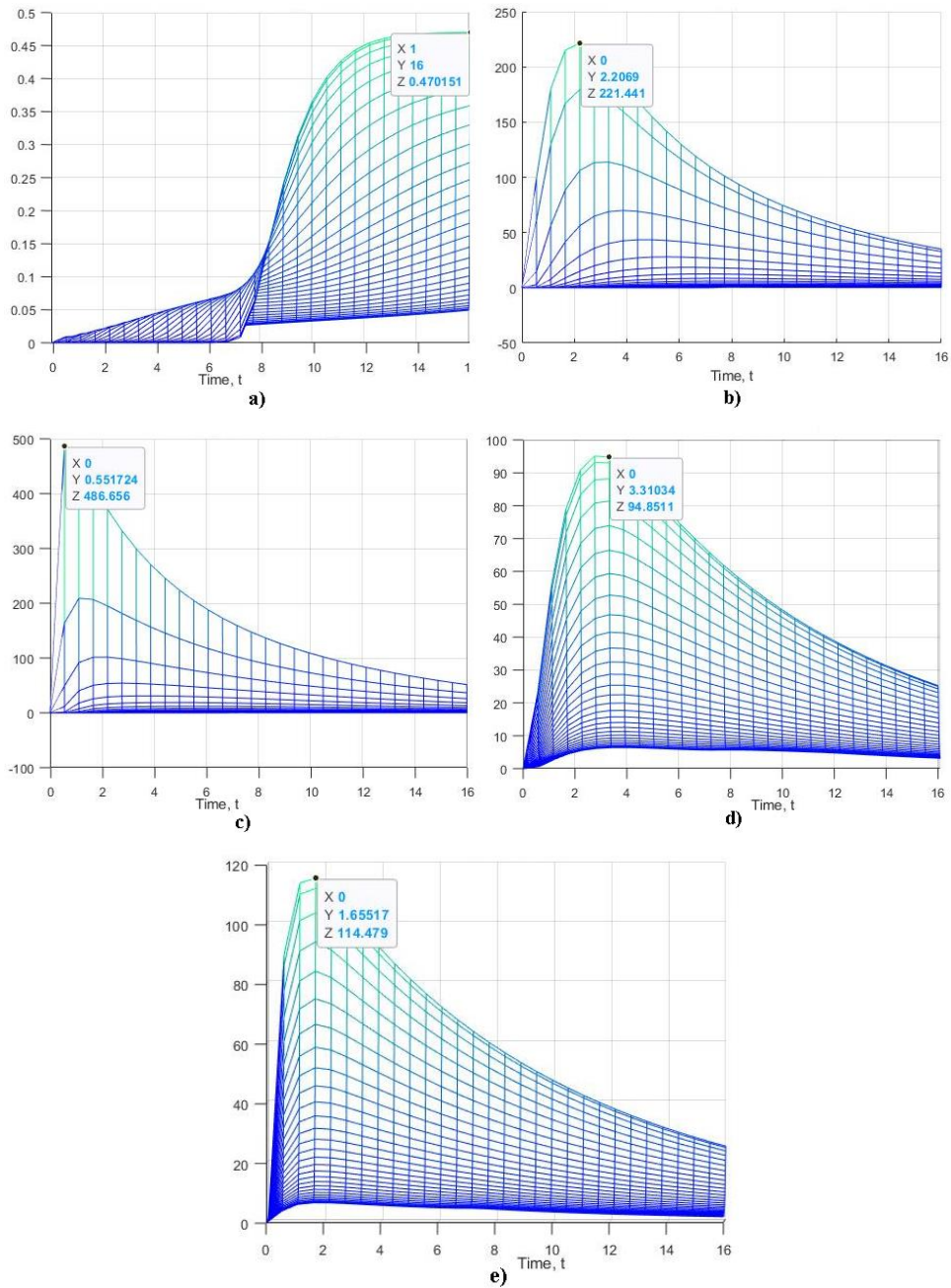


Fig. 4 Time evolution of model state variables under standard ASI conditions: a) ECM density; b) chondrocytes population density; c) MSC population density; d) BMP-2 concentration; e) FGF-1 concentration. $t=1$ roughly equivalent to 11 days

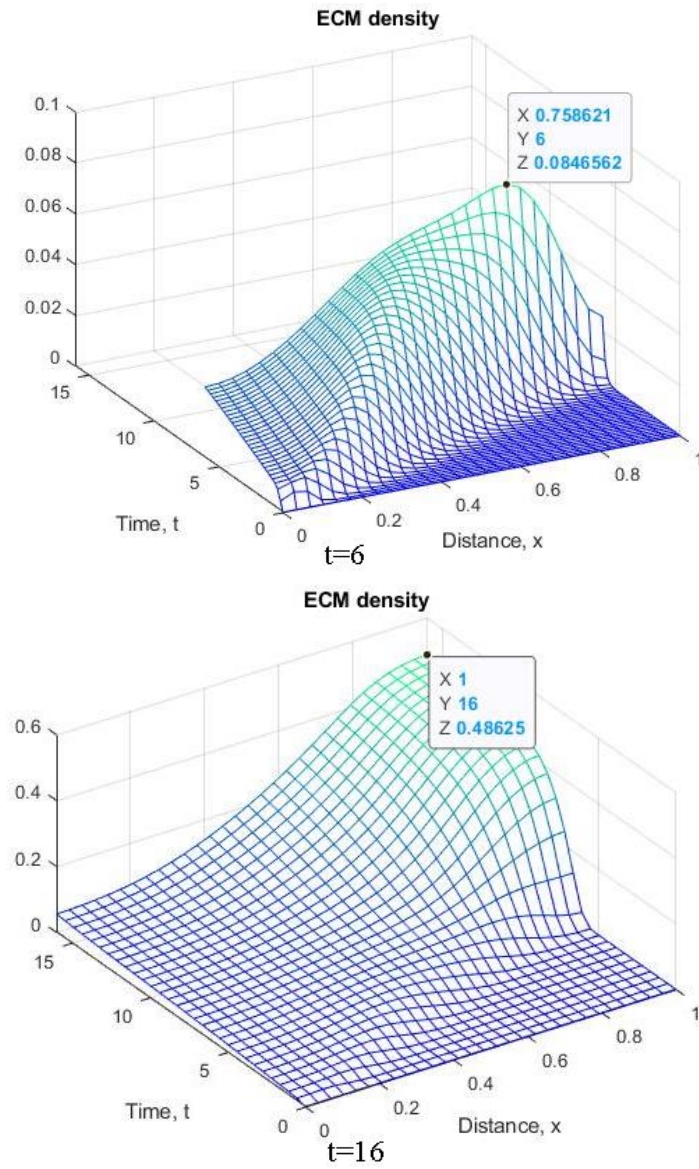


Fig. 5 The evolution of ECM density $m=m(x,t)$ of the formed tissue under conditions of regenerative rehabilitation ($t=1$ roughly equivalent to 11 days; $x=1$ equivalent to $d=2$ mm)

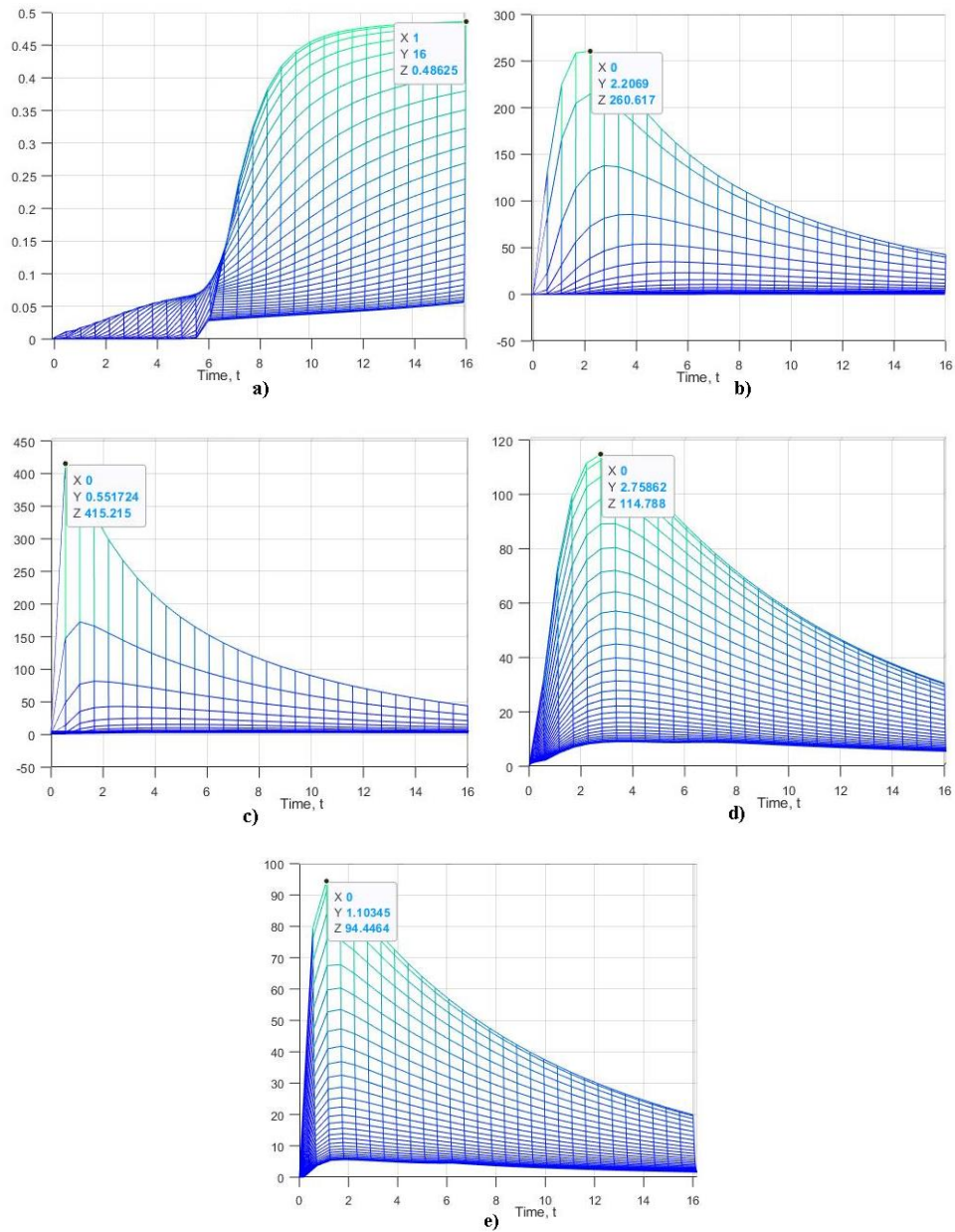


Fig. 6 Time evolution of model state variables under regenerative rehabilitation conditions: a) ECM density; b) chondrocytes population density; c) MSC population density; d) BMP-2 concentration; e) FGF-1 concentration. $t=1$ roughly equivalent to 11 days

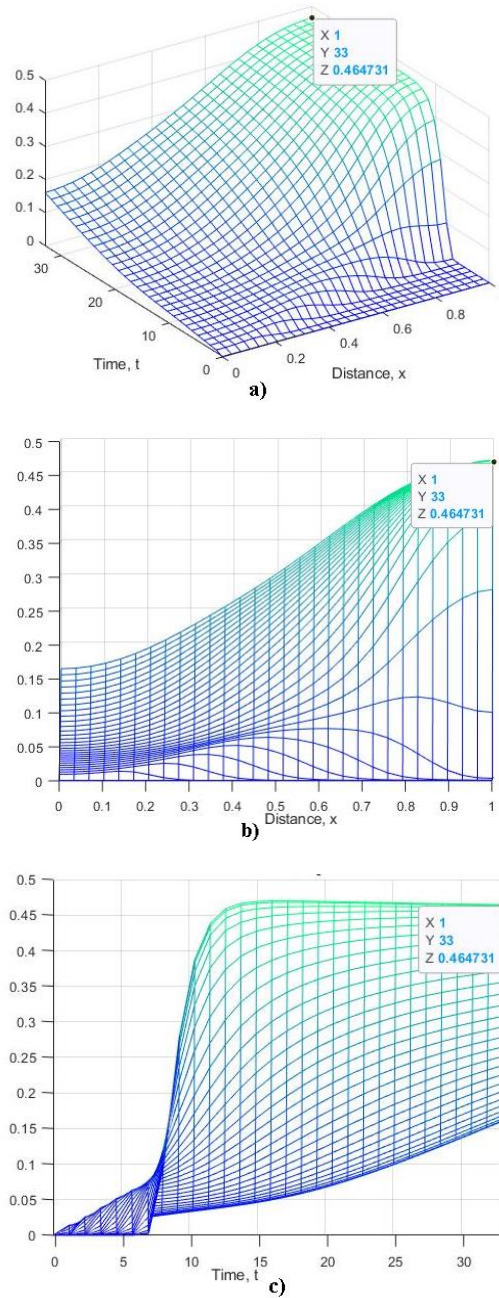


Fig. 7 The evolution of ECM density $m=m(x,t)$ of the formed tissue under standard ASI conditions for time $t = 33$: a) 3d visualization; b) visualization in the x-z plane; c) visualization in the t-z plane. $t=1$ roughly equivalent to 11 days; $x=1$ equivalent to $d=2$ mm

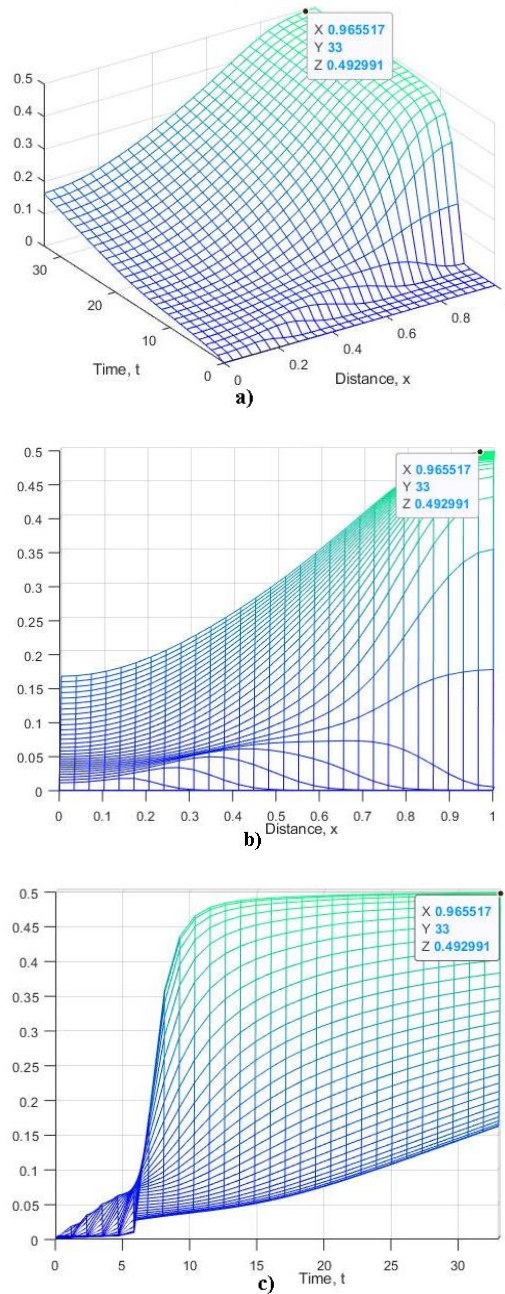


Fig. 8 The evolution of ECM density $m=m(x,t)$ of the formed tissue under conditions of regenerative rehabilitation for time $t = 33$: a) 3d visualization; b) visualization in the x - z plane; c) visualization in the t - z plane. $t=1$ roughly equivalent to 11 days; $x=1$ equivalent to $d=2$ mm

4. CONCLUSION

Increasing the intensity and quality of injuries and diseases treatment of biological tissues can be achieved by developing new technologies for regenerative rehabilitation, which, according to a large number of well-known experts, contribute to the manifestation of a synergistic effect from the combined use of advanced technologies of regenerative and rehabilitation medicine [62,63]. In this work, we aimed to show that regenerative rehabilitation can be very effective in the treatment of such a common AS disease as osteoarthritis. At the same time, it was assumed that various treatment strategies based on the combined use of cell therapy, tissue engineering constructs (scaffolds), and moderate stimulation of immature tissue can be used to treat focal AS defects. This assumption was made taking into account the results of a number of experimental *in vitro* studies published in the scientific literature, indicating the effectiveness of strategies for the regenerative rehabilitation of AS compared with conventional cell therapy. However, the results of the implementation of such strategies in experiments *in vivo* on animal models are very controversial. In this regard, the improvement of AC regenerative rehabilitation strategies that contribute to the achievement of reliable results in the treatment of osteoarthritis is an urgent scientific problem. One approach to its solution is to study various mathematical models of AC regenerative rehabilitation.

In this work, we used a simplified phenomenological biological model of regenerative rehabilitation, built on the basis of the "Diffusion-Reaction" type equations system. The study of the model was carried out by the finite element method, the effectiveness of which was confirmed by the results of many previous works [64]. Previously, a similar model was used by a number of authors to study cellular processes in various tissues under conditions of cell therapy.

Recently, many medical applications tend to use accurate geometric models of the objects under study [65]. However, in this work, a simplified geometric model was used. Nevertheless, the results of its study were generally consistent with the results of *in vivo* experiments, which led to the conclusion about its adequacy. It was shown that a change in the coefficients of the model, which determine the state of the tissue and environmental conditions, have a significant impact on the dynamics of the restored tissue structural elements, such as chondrocytes, ECM, MSC, etc. The complication of the model by taking into account a larger number of structural elements leads to a change in the dynamics of their formation, but in general it does not have a significant impact on the final result. To a large extent, its achievement depends on the parameters of the tissue and the environment, which change, including in the process of mechanical stimulation of the cartilage tissue. In this regard, the tasks of more accurate determination of diffusion coefficients, cell proliferation rates, and other parameters, depending on the qualitative and quantitative performances of mechanical stimuli applied to immature tissue, remain topical. At this stage, unfortunately, this is possible only on the basis of various more or less plausible hypotheses formulated based on the results of *in vitro* studies. Therefore, it is premature to say that based on the obtained results it is possible to plan strategies for the practical regenerative rehabilitation of AS. First, these results suggest that any strategy will be effective when stimulation of immature tissue will increase MSC and chondrocyte proliferation, increase MSC differentiation into chondrocytes, and reduce cell death. Secondly, the architectonics of the formed ECM, which mainly determines its properties, remains unknown. Thirdly, it is not clear at what time period after cell implantation stimulation of the regenerated tissue should begin and when it

should be stopped. Of no small importance are many other issues that were not addressed in this work. At the same time, it can be concluded that answers to most of these questions can be obtained as a result of the study of more complex models and more precisely defined parameters in experiments *in vivo*.

Acknowledgement: *The authors would like to thank to doctor G.D. Olinichenko for his helpful comments in preparing this paper.*

REFERENCES

1. Poliakov, A., Pakhaliuk, V., Popov, V.L., 2020, *Current trends in improving of artificial joints design and technologies for their arthroplasty*, *Frontiers in Mechanical Engineering*, 6, 4.
2. Francis, S.L., Di Bella, C., Wallace, G.G., Choong, P.F.M., 2018, *Cartilage tissue engineering using stem cells and bioprinting technology-barriers to clinical translation*, *Front Surg*, 5, 70.
3. Fox, S.A., Bedi, A., Rodeo, S.A., 2009, *The basic science of articular cartilage: structure, composition, and function*, *Sports Health*, 1, pp. 461-468.
4. Dewan, A.K., Gibson, M.A., Elisseff, J.H., Trice, M.E., 2014, *Evolution of autologous chondrocyte repair and comparison to other cartilage repair techniques*, *Biomed Res Int*, 2014(4), 272481.
5. Hong, E., Reddi, A.H., 2013, *Dedifferentiation and redifferentiation of articular chondrocytes from surface and middle zones: changes in microRNAs-221/-222, -140, and -143/145 expression*, *Tissue Eng Part A*, 19(7-8), pp. 1015-1022.
6. Dominici, M., Le Blanc, K., Mueller, I., Slaper-Cortenbach, I., Marini, F., Krause, D., Deans, R., Keating, A., Prockop, D., Horwitz, E., 2006, *Minimal criteria for defining multipotent mesenchymal stromal cells. The International Society for Cellular Therapy position statement*, *Cytotherapy*, 8(4), pp. 315-317.
7. Patel, D.M., Shah, J., Srivastava, A.S., 2013, *Therapeutic potential of mesenchymal stem cells in regenerative medicine*, *Stem Cells Int*, 2013, 2013, 496218.
8. Irion, V.H. Flanigan, D.C., 2013, *New and emerging techniques in cartilage repair: other scaffold-based cartilage treatment options*, *Oper Tech Sports Med*, 21, pp. 125-137.
9. Izadifar, Z., Chen, X., Kulyk, W., 2012, *Strategic design and fabrication of engineered scaffolds for articular cartilage repair*, *J Funct Biomater*, 3, pp. 799-838.
10. Montoya, F., Martínez, F., García-Robles, M., Balmaceda-Aguilera, C., Koch, X., Rodriguez, F., Silva-Alvarez, C., Salazar, K., Ulloa, V., Nualart, F., 2013, *Clinical and experimental approaches to knee cartilage lesion repair and mesenchymal stem cell chondrocyte differentiation*, *Biol Res*, 46(4), pp. 441-451.
11. Montaseri, A., Busch, F., Mobasheri, A., Buhmann, C., Aldinger, C., Rad, J.S., Shakibaei, M., 2011, *IGF-1 and PDGF-bb suppress IL-1b-induced cartilage degradation through down-regulation of NF- κ B signaling: involvement of Src/PI-3k/AKT pathway*, *PLoS One*, 6(12), e28663.
12. McNary, S., Athanasiou, K., Reddi, A.H., 2014, *Transforming growth factor beta-induced superficial zone protein accumulation in the surface zone of articular cartilage is dependent on the cytoskeleton*, *Tissue Eng Part A*, 20(5-6), pp. 921-929.
13. Mariani, E., Pulsatelli, L., Facchini, A., 2014, *Signaling pathways in cartilage repair*, *Int J Mol Sci*, 15, pp. 8667-8698.
14. Murphy, M.K., Huey, D.J., Hu, J.C., Athanasiou, K.A., 2015, *TGF- β 1, GDF-5, and BMP-2 stimulation induces chondrogenesis in expanded human articular chondrocytes and marrow-derived stromal cells*, *Stem Cells*, 33(3), pp. 762-773.
15. Liao, J., Hu, N., Zhou, N., Lin, L., Zhao, C., Yi, S., Fan, T., Bao, W., Liang, X., Chen, H., Xu, W., Chen, C., Cheng, Q., Zeng, Y., Si, W., Yang, Z., Huang, W., 2014, *Sox9 potentiates BMP2-induced chondrogenic differentiation and inhibits BMP2-induced osteogenic differentiation*, *PLoS One*, 9(2), e89025.
16. Li, X., Su, G., Wang, J., Zhou, Z., Li, L., Liu, L., Guan, M., Zhang, Q., Wang, H., 2013, *Exogenous bFGF promotes articular cartilage repair via up-regulation of multiple growth factors*, *Osteoarthritis Cartilage*, 21(10), pp. 1567-1575.
17. Lu, C.H., Yeh, T.S., Yeh, C.L., Fang, Y.D., Sung, L.Y., Lin, S.Y., Yen, T.C., Chang, Y.H., Hu, Y.C., 2014, *Regenerating cartilages by engineered ASCs: Prolonged TGF-(β)3/BMP-6 expression improved articular cartilage formation and restored zonal structure*, *Mol Ther*, 22(1), pp. 186-195.
18. Reyes, R., Delgado, A., Solis, R., Sanchez, E., Hernandez, A., Roman, J.S., Evora, S., 2014, *Cartilage repair by local delivery of transforming growth factor- β 1 or bone morphogenetic protein-2 from a novel, segmented polyurethane/poly(lactic-co-glycolic) bilayered scaffold*, *J Biomed Mater Res A*, 102(4), pp. 1110-1120.

19. Popov, V.L., Poliakov, A.M., Pakhaliuk, V.I., 2021, *Synovial joints. Tribology, regeneration, regenerative rehabilitation and arthroplasty*, *Lubricants*, 9(2), 15.
20. Mow, V.C., Gu, W., Chen, F.H., 2005, *Structure and Function of Articular Cartilage and Meniscus*, In *Basic Orthopaedic Biomechanics and Mechano-Biology*, 3rd ed., Mow, V.C., Huiskes, R., eds., Lippincott Williams and Wilkins: Philadelphia, PA, USA, pp. 181-258.
21. Mow, V.C., Kuei, S.C., Lai, W.M., Armstrong, C.G., 1980, *Biphasic creep and stress relaxation of articular cartilage in compression? Theory and experiments*, *J Biomech Eng*, 102(1), pp. 73-84.
22. Biot, M.A., 1941, *General Theory of Three-Dimensional Consolidation*, *Journal of Applied Physics*, 12, pp. 155-164.
23. Biot, M.A., 1956, *Theory of Propagation of Elastic Waves in a Fluid-Saturated Porous Solid. I. Low-Frequency Range*, *J of the Acoustical Soc. of America*, 28, pp. 168-178.
24. Blewis, M.E., Nugent-Derfus, G.E., Schmidt, T.A., Schumacher, B.L., Sah, R.L., 2007, *A model of synovial fluid lubricant composition in normal and injured joints*, *Eur Cell Mater*, 6(13), pp. 26-39.
25. Rullmann, J.A., Struemper, H., Defranoux, N.A., Ramanujan, S., Meeuwisse, C.M.L., van Elsas, A., 2005, *Systems biology for battling rheumatoid arthritis: application of the Entelos PhysioLab platform*, *Syst Biol (Stevenage)*, 152(4), pp. 256-262.
26. Willett, N.J., Boninger, M.L., Miller, L.J., 2020, *Taking the next steps in regenerative rehabilitation: establishment of a new interdisciplinary field*, *Arch Phys Med Rehabil*, 101(5), pp. 917-923.
27. Rando, T.A., Ambrosio, F., 2018, *Regenerative rehabilitation: applied biophysics meets stem cell therapeutics*, *Cell Stem Cell*, 22(3), pp. 306-309.
28. Cheuy, V., Picciolini, S., Bedoni, M., 2020, *Progressing the field of regenerative rehabilitation through novel interdisciplinary interaction*, *NPJ Regen Med*, 5, 16.
29. Li, K., Zhang, C., Qiu, L., Gao, L., Zhang, X., 2017, *Advances in application of mechanical stimuli in bioreactors for cartilage tissue engineering*, *Tissue Eng Part B: Rev*, 2017, 23, pp. 399-411.
30. Salinas, E.Y., Hu, J.C., Athanasiou, K., 2018, *A guide for using mechanical stimulation to enhance tissue-engineered articular cartilage properties*, *Tissue Eng Part B: Rev*, 24, pp. 345-358.
31. Saadat, E., Lan, H., Majumdar, S., Rempel, D.M., King, K.B., 2006, *Long-term cyclical in vivo loading increases cartilage proteoglycan content in a spatially specific manner: an infrared microspectroscopic imaging and polarized light microscopy study*, *Arthritis Res Ther*, 8(5), R147.
32. Hyttinen, M.M., Arokoski, J.P., Parkkinen, J.J., Lammi, M.J., Lapveteläinen, T., Mauranen, K., Király, K., Tammi, M.I., Helminen, H.J., 2001, *Age matters: collagen birefringence of superficial articular cartilage is increased in young guinea-pigs but decreased in older animals after identical physiological type of joint loading*, *Osteoarthritis Cartilage*, 9(8), pp. 694-701.
33. Neu, C.P., Khalafi, A., Komvopoulos, K., Schmid, T.M., Reddi, A.H., 2007, *Mechanotransduction of bovine articular cartilage superficial zone protein by transforming growth factor beta signaling*, *Arthritis Rheum*, 56(11), pp. 3706-3714.
34. Jortikka, M.O., Inkinen, R.I., Tammi, M.I., Parkkinen, J., Haapala, J., Kiviranta, I., Helminen, H., Lammi, M., 1997, *Immobilisation causes longlasting matrix changes both in the immobilised and contralateral joint cartilage*, *Ann Rheum Dis*, 56(4), pp. 255-261.
35. Arokoski, J.P., Jurvelin, J.S., Väättäinen, U., Helminen, H.J., 2000, *Normal and pathological adaptations of articular cartilage to joint loading*, *Scand J Med Sci Sports*, 10(4), pp. 186-198.
36. Grodzinsky, A.J., Levenston, M.E., Jin, M., Frank, E.H., 2000, *Cartilage tissue remodeling in response to mechanical forces*, *Annu Rev Biomed Eng*, 2, pp. 691-713.
37. Li, Z., Yao, S.J., Alini, M., Stoddart, M.J., 2010, *Chondrogenesis of human bone marrow mesenchymal stem cells in fibrin-polyurethane composites is modulated by frequency and amplitude of dynamic compression and shear stress*, *Tissue Eng*, 16, pp. 575-584.
38. Fahy, N., Alini, M., Stoddart, M.J., 2018, *Mechanical stimulation of mesenchymal stem cells: implications for cartilage tissue engineering*, *J Orthop Res*, 36, pp. 52-63.
39. Kasper, G., Dankert, N., Tuischer, J., Hoefl, M., Gaber, T., Glaeser, J.D., Zander, D., Tschirschmann, M., Thompson, M., Matziolis, G., Duda, G.N., 2007, *Mesenchymal stem cells regulate angiogenesis according to their mechanical environment*, *Stem Cells*, 25, pp. 903-910.
40. Albro, M.B., Nims, R.J., Cigan, A.D., Yeroushalmi, K.J., Alliston, T., Hung, C.T., Ateshian, G.A., 2013, *Accumulation of exogenous activated TGF- β in the superficial zone of articular cartilage*, *Biophys J*, 2013, 104(8), pp. 1794-1804.
41. Madej, W., van Caam, A., Blaney Davidson, E.N., van der Kraan, P.M., Buma, P., 2014, *Physiological and excessive mechanical compression of articular cartilage activates Smad2/3P signaling*, *Osteoarthritis Cartilage*, 22(7), pp. 1018-1025.
42. Albro, M.B., Nims, R.J., Cigan, A.D., Yeroushalmi, K.J., Shim, J.J., Hung, C.T., Ateshian, G.A., 2013, *Dynamic mechanical compression of devitalized articular cartilage does not activate latent TGF- β* , *J Biomech*, 46(8), pp. 1433-1439.

43. Fitzgerald, J.B., Jin, M., Dean, D., Wood, D.J., Zheng, M.H., Grodzinsky, A.J., 2004, *Mechanical compression of cartilage explants induces multiple time-dependent gene expression patterns and involves intracellular calcium and cyclic AMP*, J Biol Chem, 279(19), pp. 19502-19511.
44. Liu, Y., Shah, K.M., Luo, J., 2021, *Strategies for articular cartilage repair and regeneration*, Front Bioeng Biotechnol, 9, 770655.
45. Vermolen, F.J., Javierre, E., 2009, *A suite of continuum models for different aspects in wound healing*, in: Gefen, A. (eds) Bioengineering Research of Chronic Wounds, SMTEB, 1, Springer, Berlin, Heidelberg, pp. 127-168.
46. Lutianov, M., Naire, S., Roberts, S., Kuiper, J.H., 2011, *A mathematical model of cartilage regeneration after cell therapy*, J Theor Biol, 289, pp. 136-150.
47. Campbell, K., Naire, S., Kuiper, J.H., 2019, *A mathematical model of cartilage regeneration after chondrocyte and stem cell implantation - I: the effects of growth factors*, J Tissue Eng, 10, 2041731419827791.
48. Campbell, K., Naire, S., Kuiper, J.H., 2019, *A mathematical model of cartilage regeneration after chondrocyte and stem cell implantation - II: the effects of co-implantation*, J Tissue Eng, 10, 2041731419827792.
49. Bailón-Plaza, A., van der Meulen, M.C., 2001, *A mathematical framework to study the effects of growth factor influences on fracture healing*, J Theor Biol, 212(2), pp. 191-209.
50. Obradovic, B., Meldon, J., Freed, L., Vunjak-Novakovic, G., 2000, *Glycosaminoglycan deposition in engineered cartilage: experiments and mathematical model*, Aiche Journal, 46, pp. 1860-1871.
51. Zhou, S., Cui, Z., Urban, J.P., 2004, *Factors influencing the oxygen concentration gradient from the synovial surface of articular cartilage to the cartilage-bone interface: a modeling study*, Arthritis Rheum, 50(12), pp. 3915-3924.
52. Isaksson, H., Wilson, W., van Donkelaar, C.C., 2006, *Comparison of biophysical stimuli for mechano-regulation of tissue differentiation during fracture healing*, J Biomech, 39(8), pp. 1507-1516.
53. Prendergast, P.J., Huiskes, R., Søballe, K., 1997, *Biophysical stimuli on cells during tissue differentiation at implant interfaces*, J Biomech, 30(6), pp. 539-48.
54. Bailón-Plaza, A., van der Meulen, M.C., 2003, *Beneficial effects of moderate, early loading and adverse effects of delayed or excessive loading on bone healing*, J Biomech, 36(8), pp. 1069-1077.
55. Lacroix, D., Prendergast, P.J., 2002, *A mechano-regulation model for tissue differentiation during fracture healing: analysis of gap size and loading*, J Biomech, 35(9), pp. 1163-1171.
56. Andreykiv, A., van Keulen, F., Prendergast, P.J., 2008, *Simulation of fracture healing incorporating mechanoregulation of tissue differentiation and dispersal/proliferation of cells*, Biomech Model Mechanobiol, 7(6), pp. 443-61.
57. Huiskes, R., Van Driel, W.D., Prendergast, P.J., Søballe, K., 1997, *A biomechanical regulatory model for periprosthetic fibrous-tissue differentiation*, J Mater Sci Mater Med, 8(12), pp. 785-788.
58. Kaspar, D., Seidl, W., Neidlinger-Wilke, C., Beck, A., Claes, L., Ignatius, A., 2002, *Proliferation of human-derived osteoblast-like cells depends on the cycle number and frequency of uniaxial strain*, J Biomech, 35(7), pp. 873-880.
59. Kaspar, D., Seidl, W., Neidlinger-Wilke, C., 2000, *Dynamic cell stretching increases human osteoblast proliferation and C1CP synthesis but decreases osteocalcin synthesis and alkaline phosphatase activity*, J Biomech, 33(1), pp. 45-51.
60. Zhang, Z.J., Huckle, J., Francomano, C.A., Spencer, R.G., 2003, *The effects of pulsed low-intensity ultrasound on chondrocyte viability, proliferation, gene expression and matrix production*, Ultrasound Med Biol, 29(11), pp. 1645-1651.
61. Wu, Q.Q., Chen, Q., 2000, *Mechanoregulation of chondrocyte proliferation, maturation, and hypertrophy: ion-channel dependent transduction of matrix deformation signals*, Exp Cell Res, 256(2), pp. 383-391.
62. Rose, L.F., Wolf, E.J., Brindle, T., Cernich, A., Dean, W.K., Dearth, C.L., Grimm, M., Kusiak, A., Nitkin, R., Potter, K., Randolph, B.J., Wang, F., Yamaguchi, D., 2018, *The convergence of regenerative medicine and rehabilitation: federal perspectives*, NPJ Regen Med, 3, 19.
63. Mohammadkhah, M., Marinkovic, D., Zehn, M., Checa, S., 2019, *A review on computer modeling of bone piezoelectricity and its application to bone adaptation and regeneration*, Bone, 127, pp. 544-555.
64. Eremina, G., Smolin, A., Martyshina, I., 2022, *Convergence analysis and validation of a discrete element model of the human lumbar spine*, Reports in Mechanical Engineering, 3(1), pp. 62-70.
65. Stojkovic, M., Veselinovic, M., Vitkovic, N., Marinkovic, D., Trajanovic, M., Arsic, S., Mitkovic, M., 2018, *Reverse modelling of human long bones using T-splines-case of tibia*, Tehnicki Vjesnik, 25(6), pp. 1753-1760.

APPENDIX A
PARAMETERS OF REPAIR MODEL / AC FOCAL DEFECT REGENERATIVE REHABILITATION

| Parameter | Parameter value | Parameter dimension | Dimensionless parameter value |
|---|--|--|-------------------------------|
| C_S – MSC density | $C_S = C_S(x, t)$ | $\frac{cells}{mm^3}$ | - |
| C_C – chondrocyte density | $C_C = C_C(x, t)$ | $\frac{cells}{mm^3}$ | - |
| m – ECM density | $m = m(x, t)$ | $\frac{g}{mm^3}$ | - |
| n – nutrient concentration | $n = n(x, t)$ | $\frac{moles}{mm^3}$ | - |
| g – FGF-1 concentration | $g = g(x, t)$ | $\frac{g}{mm^3}$ | - |
| b – BMP-2 concentration | $b = b(x, t)$ | $\frac{g}{mm^3}$ | - |
| D_S – MSC random motility (diffusion) coefficient | $D_S = D_{S0} \frac{m}{m^2+m_1^2}$ | $\frac{mm^2}{hour}$ | - |
| D_{S0} – MSC diffusion constant | $D_{S0} = 2m_1D_S^* = 7.2 \times (10^{-9} \div 10^{-8})$ | $\frac{mm^2}{hour} \cdot \frac{g}{mm^3}$ | 0.001 – 0.01 |
| D_S^* – maximum MSC diffusion coefficient | $D_S^* = 3.6 \times (10^{-4} \div 10^{-3})$ | $\frac{mm^2}{hour}$ | - |
| D_C – chondrocyte random motility (diffusion) coefficient | $D_C = D_{C0} \frac{m}{m^2+m_2^2}$ | $\frac{mm^2}{hour}$ | - |
| D_{C0} – chondrocyte diffusion constant | $D_{C0} = 2m_1D_C^*$ | $\frac{mm^2}{hour} \cdot \frac{g}{mm^3}$ | 0.001 |
| D_C^* – maximum chondrocyte diffusion coefficient | $D_C^* = 3.6 \times (10^{-4} \div 10^{-3})$ | $\frac{mm^2}{hour}$ | - |
| D_n – nutrient diffusion coefficient | $D_n = 4.6$ | $\frac{mm^2}{hour}$ | 100 - 300 |
| D_m – ECM diffusion coefficient | $D_m = 2.5 \times 10^{-5}$ | $\frac{mm^2}{hour}$ | 0.001 – 0.01 |
| D_g – FGF-1 diffusion coefficient | $D_g = 2 \times 10^{-3}$ | $\frac{mm^2}{hour}$ | 1.14 |
| D_b – BMP-2 diffusion coefficient | $D_b = 2 \times 10^{-3}$ | $\frac{mm^2}{hour}$ | 1.14 |
| p_1 – MSC proliferation rate | $p_1 = A_m \left(1 - \frac{C_S}{C_{Smax}}\right);$ $A_m = p_{10} \frac{m}{m^2+m_2^2};$ $C_{Smax} = C_{Smax0} \left(1 - \frac{m}{m_{max}}\right)$ | $\frac{cell}{hour}$ - | - |
| p_{10} – MSC proliferation constant | $p_{10} = 2m_2p_1^* = 4 \times 10^{-6}$ | $\frac{g}{mm^3} \cdot \frac{1}{hour}$ | 12 |
| p_1^* – maximum MSC proliferation rate | $p_1^* = 0.2$ | $\frac{cell}{hour}$ | - |
| C_{Smax0} – maximum MSC density | $C_{Smax0} = 0 \div 10^6$ | $\frac{Nc}{mm^3}$ | 0.6 |
| m_1 – reference ECM density | $m_1 = 10^{-5}$ (assumed $m_{max}/10$) | $\frac{g}{mm^3}$ | 0.1 |
| m_2 – reference ECM density | $m_2 = 10^{-5}$ (assumed $m_{max}/10$) | $\frac{g}{mm^3}$ | 0.1 |

| | | | |
|--|--|---------------------------------------|-------------|
| m_{max} – maximum ECM density | $m_{max} = 10^{-4}$ | $\frac{g}{mm^3}$ | - |
| p_2 – MSC differentiation rate | $p_2 = 3.75 \times 10^{-3}$ | $\frac{1}{hour}$ | 1.0 |
| p_3 – MSC death rate | $p_3 = 3.75 \times 10^{-3}$ | $\frac{1}{hour}$ | 1.0 |
| p_4 – chondrocyte proliferation rate | $p_4 = B_m \left(1 - \frac{C_c}{C_{Cmax}}\right);$ $B_m = p_{4_0} \frac{m}{m^2 + m_2^2} + p_{4_{00}} \frac{g}{g + g_0};$ $C_{Cmax} = C_{Cmax0} \left(1 - \frac{m}{m_{max}}\right)$ | $\frac{1}{hour}$ | - |
| g_0 – FGF-1 reference concentration | $g_0 = 10^{-10}$ | $\frac{g}{mm^3}$ | - |
| p_{4_0} – chondrocyte proliferation constant | $p_{4_0} = 2m_2 p_4^* = 4 \times 10^{-9}$ | $\frac{g}{mm^3} \cdot \frac{1}{hour}$ | 0.012 |
| p_4^* – maximum chondrocyte proliferation rate | $p_4^* = 2 \times 10^{-4}$ | $\frac{1}{hour}$ | - |
| $p_{4_{00}}$ – chondrocyte proliferation rate (from FGF-1) | $p_{4_{00}} = 2 \times 10^{-4}$ | $\frac{1}{hour}$ | 0.012 |
| C_{Cmax0} – maximum chondrocyte density | $C_{Cmax0} = 0 \div 10^6$ | $\frac{Nc}{mm^3}$ | 0.4 |
| $H(n - n_1)$ – Heaviside function | $H(n - n_1) = \begin{cases} 0, n \leq n_1 \\ 1, n > n_1 \end{cases}$ | - | - |
| n_1 – critical nutrient concentration | $n_1 = 9.5 \times 10^{-12}$ | $\frac{Nm}{mm^3}$ | 0.1 |
| n_0 – threshold nutrient concentration | $n_0 = 2.3 \times 10^{-11}$ | $\frac{Nm}{mm^3}$ | 0.24 – 0.81 |
| $H(C_S - C_{S_0})$ – Heaviside function | $H(C_S - C_{S_0}) = \begin{cases} 0, C_S \leq C_{S_0} \\ 1, C_S > C_{S_0} \end{cases}$ | - | - |
| C_{S_0} – MSC threshold density | $C_{S_0} = (C_{S_{0max}} - C_{S_{0min}})e^{-\alpha b} + C_{S_{0min}}$ | $\frac{Nc}{mm^3}$ | - |
| $C_{S_{0max}}$ – maximum threshold MSC density | $\frac{C_{total,max0}}{2}$ | $\frac{Nc}{mm^3}$ | 0.35 |
| $C_{S_{0min}}$ – minimum threshold MSC density | $0.9C_{S_{0max}}$ | $\frac{Nc}{mm^3}$ | 0.315 |
| $H(n_1 - n)$ – Heaviside function | $H(n_1 - n) = \begin{cases} 0, n_1 \leq n \\ 1, n_1 > n \end{cases}$ | - | - |
| p_5 – chondrocyte death rate | $p_5 = 3.75 \times 10^{-3}$ | $\frac{1}{hour}$ | 1 |
| p_6 – nutrient uptake constant by MSC | $p_6 = 1.5 \times 10^{-14}$ | $\frac{Nm}{Nc \cdot hour}$ | 10000 |
| p_7 – nutrient uptake constant by chondrocytes | $p_6 = 1.5 \times 10^{-14}$ | $\frac{Nm}{Nc \cdot hour}$ | 10000 |

| | | | |
|---|---|--|--------|
| p_8 – ECM synthesis rate | $p_8 = p_{8_0} - p_{8_1}m$ | $\frac{g}{mm^3} \cdot \frac{1}{Nc/mm^3}$ | - |
| p_{8_0} – ECM production constant | $p_{8_0} = 3.75 \times 10^{-13}$ | $\frac{hour}{mm^3} \cdot \frac{1}{Nc/mm^3} \cdot \frac{1}{hour}$ | 0 - 1 |
| $p_{8_{00}}$ – FGF-1 ECM deposition rate | $p_{8_{00}} = 0 \div 1$ | - | 0 - 1 |
| p_{8_1} – ECM degradation constant | $p_{8_1} = 3.75 \times 10^{-9}$ | $\frac{1}{mm^3} \cdot \frac{1}{hour}$ | 1 |
| p_9 – FGF-1 production constant | $p_9 = 10^{-17}$ | $\frac{g}{mm^3} \cdot \frac{1}{Nc/mm^3} \cdot \frac{1}{hour}$ | 26.67 |
| p_{11} – FGF-1 degradation rate | $p_{11} = 5.8 \times 10^{-2}$ | $\frac{1}{hour}$ | 15.4 |
| p_{12} – BMP-2 production constant | $p_{12} = 10^{-17}$ | $\frac{g}{mm^3} \cdot \frac{1}{Nc/mm^3} \cdot \frac{1}{hour}$ | 26.67 |
| p_{13} – BMP-2 degradation rate | $p_{13} = 5.8 \times 10^{-2}$ | $\frac{1}{hour}$ | 15.4 |
| $C_{total,max0}$ – maximum total cell density | $C_{total,max0} = \left(1 - \frac{m}{m_{max}}\right)^{-1} (C_{Smax} + C_{Cmax}) = 10^6$ | $\frac{Nc}{mm^3}$ | - |
| α – threshold stem cell density reduction factor | $\alpha = 10^{10}$ | $\frac{1}{g/mm^3}$ | 100 |
| γ – FGF-1 flux coefficient | $\gamma = 10^{-2}$ | $\frac{mm}{hour}$ | 0.01 |
| χ – BMP-2 flux coefficient | $\chi = 10^{-2}$ | $\frac{hour}{mm}$ | 1 |
| b_0 – BMP-2 reference concentration | $b_0 = 10^{-10}$ | $\frac{hour}{mm^3} \cdot \frac{g}{mm^3}$ | - |
| $C_S^{(0)}$ – initial MSC density | $C_S^{(0)} = 2.5 \times 10^5$ (based on 10^6 cells in $20\text{ mm} \times 20\text{ mm} \times 10\text{ }\mu\text{m}$ volume) | $\frac{Nc}{mm^3}$ | 0.25 |
| $C_C^{(0)}$ – initial chondrocytes density | $C_C^{(0)} = 10^2$ ($10^{-2}\%$ of total cell density) | $\frac{Nc}{mm^3}$ | 0.0001 |
| N_0 – initial nutrient concentration | $N_0 = (2.85 \div 9.5)10^{-11}$ | $\frac{Nm}{mm^3}$ | - |
| m_3 – initial ECM density | $m_3 = 10^{-8}$ (assumed $m_{max}/10^4$) | $\frac{g}{mm^3}$ | 0.0001 |
| g_{init} – initial FGF-1 concentration | $g_{init} = 10^{-12}$ | $\frac{g}{mm^3}$ | 0.01 |
| b_{init} – initial BMP-2 concentration | $g_{init} = 10^{-12}$ | $\frac{g}{mm^3}$ | 0.01 |